International Journal of Engineering & Technology, 7 (4.14) (2018) 356-360

International Journal of Engineering & Technology

Website: www.sciencepubco.com/index.php/IJET

Research paper

Effects of Coil Pitch Spacing on Heat Transfer Performance of Nanofluid Turbulent Flow through Helical Microtube Heat Exchanger

A.H. Rasheed [1]*, H. Alias[1], S.D. Salman[2]

[1]*Chemical Engineering Department, Faculty of Chemical and Energy Engineering, Universiti Teknologi Malaysia, Johor, Malaysia*
[2]*Al- Khwarizmi College of Engineering, University of Baghdad, Baghdad, Iraq*
**Corresponding author E-mail: adnan_akeedy@yahoo.com*

Abstract

This article provides Numerical simulation on forced convective heat transfer performance of Nanofluid flowing through copper helical microtube of inner diameter of 1.5 mm with different pitch using ANSYS-FLUENT 18.0. The simulation was performed for water, CuO/water, Al_2O_3/water Nanofluid with 1-2% volume concentration and different pitch of microtube (10, 14 and 18 mm) for turbulent flow regime of Reynolds number varied 5000 to 20000 and governing equations of mass, momentum and heat transfer were solved simultaneously, using the k-e two equations turbulence model. Based on the obtained results, regardless of the concentrations used, the nanofluids exhibited a higher transfer rate than water. This is mainly attributed to the nanoparticles that are in the used nanofluids. The friction factor and the heat transfer rate were enhanced considerably due to the shape and size of the tube, which in this case is a helical microtube. Moreover, the maximum heat transfer performance has been conducted by Al_2O_3/water Nanofluid with 2% volume concentration and microtube pitch of 18 mm.

Keywords: *Heat transfer enhancements, Helical micro coil Nanofluids, Mathematical model*

1. Introduction

Heat Transfer Enhancement or Intensification is a technique in heat a transfer system which refers to thermal performance improvement. The effect of the improvements that is caused by the use of these techniques, leads to heat transfer systems to be smaller in size, and cheaper when it comes to the cost. These systems are widely used in many industries such as transportations, air-conditioning systems, cooling systems, nuclear reactors, cooling of electronic parts, space and defense, optical and biomedical applications. [1].

In general, the enhancement techniques classified into two categories. The nature of this categorization is based on whether or not these techniques have a dependency or need on external power. Techniques that are dependent on the external source are known as active techniques, while those that do not have such dependency are known as passive techniques. Examples of active techniques can be described as electric fields, jet impingement, acoustic or surface vibration, while passive type technique examples are types of surfaces, (rough, extended and treated), fluid additives (Nanofluids) and special surface geometries to the flow channel by incorporating inserts. Two or more passive and/or active techniques in the context of the compound technique may be used to produce an enhancement higher than each technique operating individually [2, 3].

Several research studies have been implemented experimentally and numerically on heat transfer enhancement using different types of nanofluids with flow conditions categorized as turbulent. Xuan and Li [4] performed an experiment in a turbulent flow environment, all the while measuring the convective heat transfer using a uniform heat flux tube using varying concentration of Cu nanofluid which where somewhere between 0 and 2%. The results indicated a significant improvement of heat transfer coefficient, while Nusselt number also saw some enhancement when compared to the base fluid with the same Reynolds number tested. Maïga et al. [5] have implemented a numerical investigation on both saturated water and aluminum oxide (Al_2O_3) as the nanofluid. The investigation was identifying the hydrodynamics of the situation all the while analyzing the effect of the turbulent flow. This numerical experimentation was performed using various concentration levels using a uniform wall heat flux boundary condition. The results indicated a direct correlation between the concentration of the particles in the fluid, and the heat transfer coefficient.

Namburu et al. [6] numerically analyzed three different nanofluids. These nanofluids were mixed in water and ethylene glycol in a heat flux tube of the constant form. These nanofluids were silicon dioxide, aluminum oxide, and copper (II) oxide. Based on the results, the nanoparticles that had a smaller diameter, were more viscous, and their Nusselt number was comparatively higher. This also affected the heat transfer coefficient and the pressure loss, as they both increased with the increase in concentration value. With the concentration of 6%, CuO nanofluid presents higher heat transfer performance, followed by Al_2O_3 and SiO_2. Diluted nanofluids with CuO nanoparticles of volume fractions less than 0.3% were experimentally investigated by Fotukian and Nasr Esfahany [7]. Their measurements indicated that by adding copper (II) oxide to the mix of the base fluid, there is a significant increase in heat transfer coefficient. The values were then compared with the correlation of Buongiorno [8]. Demir et al. [9] performed and experiment numerically via a simulation, on nanofluids convection flows in a constant tube wall temperature

with water/TiO_2 for study validation and Al_2O_3/water with various volume concentrations (1% and 4%) for the simulation. The results indicated that the results were agreement with a previous experiment performed by Duangthongsuk and Wongwises [10], which was the improvement of heat transfer enhancement using the water/TiO_2. Sajadi and Kazemi [11] performed a similar experiment which mainly focused on the behavior of the TiO_2/water. It was discovered that heat transfer rate is enhanced at certain concentration while comparing it with the base fluid of water. Kayhani et al. [12] has an experiment in a similar vein on the same nanofluid. This time, different concentration were tested, which indicated an improvement in the heat transfer coefficient as well as the volume without any great impact on the pressure drop or the Nusselt number.
In addition, there are several other studies that focus on flow pulsation on heat transfer enhancement. Numerically, Xiao et al. [13] performed an experiment which used the microtube and gas as the element within the tube. A second-order slip flow, was used as well in order to satisfy the iso flux thermal boundary condition. Based on the results from the simulation, the second-order model rarefield flow heat transfer effects were reduced. An experimental investigation performed by Koo and Kleinstreuer [14], focused on the effects of water, methanol and is-propanol on microtube and microchannel. Based on the observed results, a negative correlation occurred between the viscous dissipation and system size, as the latter decreased, the effect of the viscous dissipation on the friction factor increased. Although this study was focused on liquids, another used gaseous slip in a numerical experiment [15]. The setting revolved around the use of an infinite microtube, while the boundary conditions varried. A negative correlation was observed between the Nusselt number and Knudsen number, while a positive correlation was set for the Nusselt number and Peclet number. Another numerical investigation by Wang and Wang [16] focused on microtubes as well, however in this research the wall roughness was of main concern, particularly on a 3D scale and its effects on the laminar flow. The results showed a negative correlation between the Reynolds number and disturb areas of flow field, as the latter became larger, the first decreased in value. A research by Aziz and Niedbalski [17] simulated microtube with diluted gas flow. This simulation and numerical experiment was conducted based on the first and second order slip, and the results showed that as the fluid flowed through the cooler sections of the microtube, the value of the Nusselt number decreased.

2. Numerical model

2.1. Geometry and the governing equations

The 3-D Navier–Stokes and energy equations were used to describe the flow and heat transfer in the microtube. Fig. 1 and 2 present the computational and mesh domain for microtube model. In the Cartesian coordinates the governing equations are as follows:

Continuity equation: $\frac{\partial u}{\partial x}+\frac{\partial v}{\partial y}+\frac{\partial w}{\partial z}=0$ (1)

Momentum:

x-direction equation :

$$u\frac{\partial u}{\partial x}+v\frac{\partial u}{\partial y}+w\frac{\partial u}{\partial z}=-\frac{\partial P}{\partial x}+v\left(\frac{\partial^2 u}{\partial x^2}+\frac{\partial^2 u}{\partial y^2}+\frac{\partial^2 u}{\partial z^2}\right) \quad (2)$$

y-direction equation:

$$u\frac{\partial v}{\partial x}+v\frac{\partial v}{\partial y}+w\frac{\partial v}{\partial z}=-\frac{\partial P}{\partial x}+v\left(\frac{\partial^2 v}{\partial x^2}+\frac{\partial^2 v}{\partial y^2}+\frac{\partial^2 v}{\partial z^2}\right) \quad (3)$$

z-direction equation :

$$u\frac{\partial w}{\partial x}+v\frac{\partial w}{\partial y}+w\frac{\partial w}{\partial z}=-\frac{\partial P}{\partial x}+v\left(\frac{\partial^2 w}{\partial x^2}+\frac{\partial^2 w}{\partial y^2}+\frac{\partial^2 w}{\partial z^2}\right) \quad (4)$$

where:

$\mathcal{V}$ represent the fluid kinematic viscosity ($\mathcal{V}$ = μ/ ρ)

Energy equation:

$$u\frac{\partial T}{\partial x}+v\frac{\partial T}{\partial y}+w\frac{\partial T}{\partial z}=\alpha\left(\frac{\partial^2 T}{\partial x^2}+\frac{\partial^2 T}{\partial y^2}+\frac{\partial^2 T}{\partial z^2}\right) \quad (5)$$

where:

α represent the fluid thermal diffusivity ($\alpha = k/\rho C_p$).

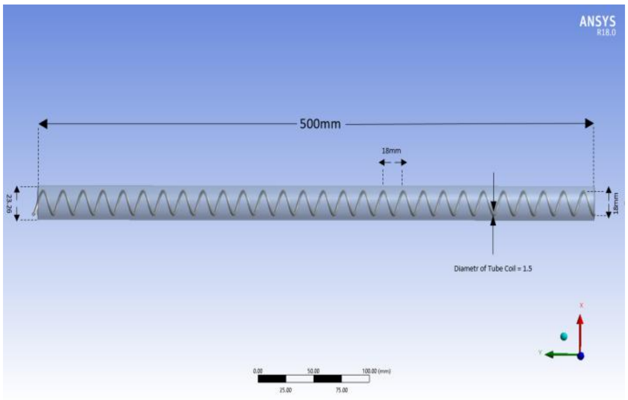

Fig. 1: Micro tube model

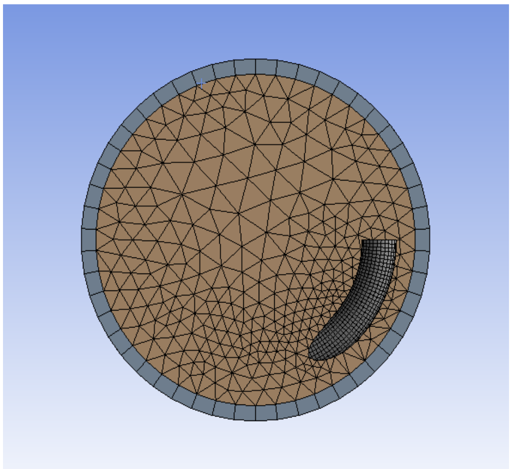

Fig. 2: Meshed Micro tube model

2.2. Thermophysical properties of nanofluids

In order to obtain the properties the used nanofluids in terms of their thermophysical nature, equation 6 through 10 were used.

For the density

The density of nanofluid ρ_{nf}can be obtained from the following equation [18]

$$\rho_{nf}=(1-\phi)\rho_f+\phi\rho_{np} \quad (6)$$

where :

ρ_f and ρ_{np} are the mass densities of the based fluid and the solid nanoparticles, respectively.

For the heat capacity

The effective heat capacity at constant pressure of nanofluid, can be calculated from the following equation [19]

$$(\rho c_p)_{nf}=(1-\phi)(\rho c_p)_f+\phi(\rho c_p)_{np} \quad (7)$$

where:

$(\rho c_p)_f$ and $(\rho c_p)_{np}$ are the heat capacities of the based fluid and the solid nanoparticles, respectively

For Effective thermal conductivity

By using Brownian motion of nanoparticles, the effective thermal conductivity can be obtained by using the following mean empirical correlation [18]

$$K_{static} = K_{static} + K_{Brownian} \quad (8)$$

$$K_{static} = K_f \left| \frac{[illegible]}{[illegible]} \right| \quad (9)$$

$$k_{Brwnian} = 5 * 10^4 \beta \phi \rho_f C_{p,f} \sqrt{\frac{KT}{[illegible]}} f(T, \phi) \quad (10)$$

where:
Boltzmann constant: $k = 1.3807 * 10^{-23} \frac{J}{K}$
Modelling, $f(T, \phi)$

$$f(T,\phi) = (2.8217 * 10^{-2} \phi + 3.917 * 10^{-3}) \left(\frac{T}{T_0}\right) + (-3.669 * 10^{-2} \phi - 3$$

For Effective viscosity
The effective viscosity can be obtained by using the following mean empirical correlation [19]

$$\mu_{eff} = \mu_f \times \frac{1}{[illegible]} \quad (11)$$

$$d_f = \left| \frac{6M}{N\pi\rho} \right|^{[illegible]} \quad (12)$$

where M is the molecular weight of base fluid, N is the Avogadro number = 6.022*10^{23} mol^{-1}, ρ_f is the mass density of the based fluid calculated at temperature T_0=293K.

2.3. Numerical method and grid testing

In order to address the issue of continuity, an approach known as finite volume was used. However, this also addresses the momentum and aforementioned energy equations, as well as the boundary conditions. As the study required a grid size for the geometry, a test known as the grid independence is used to obtain those metrics. Four different sizes were used for the grid, these were 3915382, 4287098, 4423552 and 5000000, all of which demonstrated to have only slightly affected on the Nusselt number. For this reason, the size that was ultimately used was the 4423552 as it apparently provided a better grid independent solution according to the simulation.

3. Result and discussion

3.1. Effect of Micro coil picth

The influence of micro coil pitch (10mm, 14mm, and 18mm) on Nusselt number, skin friction factor and thermal performance using water as test fluid are shown in Figs. 3, 4 and 5. Apparently from Fig. 3, micro coil with pitch 10mm exhibits higher Nusselt number than others. The reason behind this is that micro coil with pitch 10mm generates swirl flow with efficient fluid mixing nearby their alternative curveture and with tube wall. From Fig. 4, it can be seen that friction factor decreases with Reynolds number and increase with decreasing of coil pitch. This implies that the influence of nearest alternative pitch along the pipe promotes additional wall shear stress due to flow mixing between the fluid and tube wall. Fig. 5 shows the variation of thermal performance factor with Reynolds number. The values of thermal performance factor increase with Reynolds number and pitch. This is an indication of the energy saving feasibility of the micro coil when using the turbulent flow. It is also evident that the thermal performance factor for 18mm pitch value at constant Reynolds number is higher than others. This because the turbulence/swirl flow generated a long the coil as it became stronger.

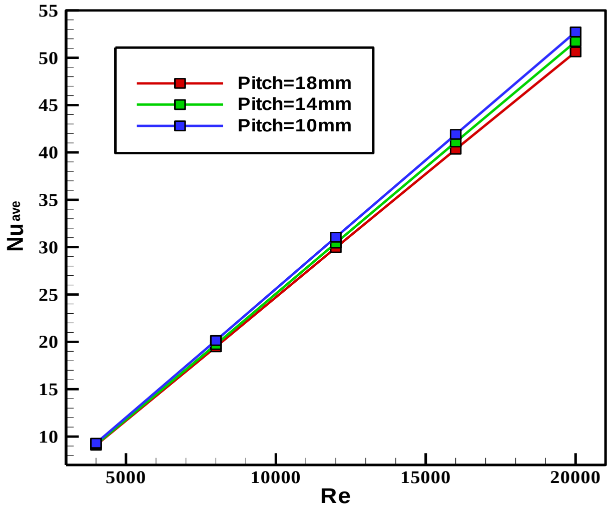

Fig. 3: Variation of the Nusselt number vs Reynolds number with différent coil pitch and diameter

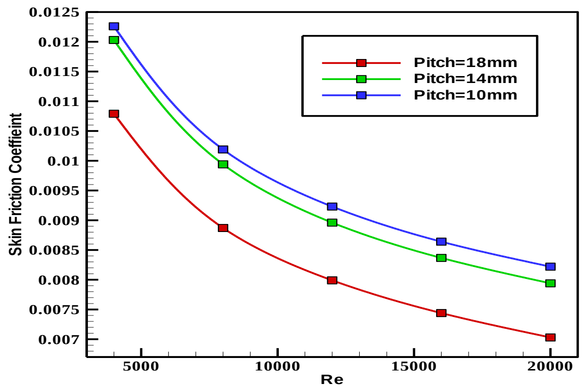

Fig. 4: Variation of the skin friction factor vs Reynolds number with différent coil pitch and diameter

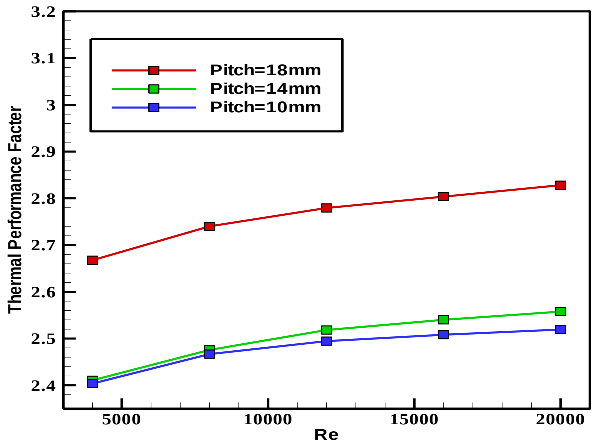

Fig. 5: Variation of the thermal performance factor vs Reynolds number with different coil pitch and diameter

3.2. Effect of nanoparticle concentrations

Variations of heat transfer coefficient and friction factor versus Reynolds number for water, Al_2O_3 and CuO nanofluids of 1% and 2% volume concentration by fixing the coil pitch value (18mm) are shown in Figs. 6 and 7. Evidently, Fig. 6 shows that the combined use of nanofluid with micro coil produces further augment in heat transfer coefficient than water. The simultaneous use of nanofluid with coil increases the thermal conductivity and viscosity of working fluid as well as increasing swirl flow path. Thus, greater fluid mixing and higher heat transfer coefficient are produced. Eventually, Al_2O_3 nanofluid with 2% volume concentration offered a higher heat transfer coefficient compared with the others. Figure 7 demonstrates a negative correlation between the Reynolds number and the friction factor, regardless of the fluid used, since both the water and different nanoparticles seem to exhibit the same effect. As Reynolds number is increased, the friction coefficient is reduced. This phenomenon is attributed to the increase in viscosity and concentration, which in turn increase the wall shear stress. As it can be seen, the low viscocity has contributed in making water lower than other nanofluids when it comes shear stress value. An increase in pressure drop has also been noted to correlate positively with viscosity. However, the simulated results seem to indicate no correlation between nanofluid concentration and pressure drop, as the friction factor exhibits no significant change.

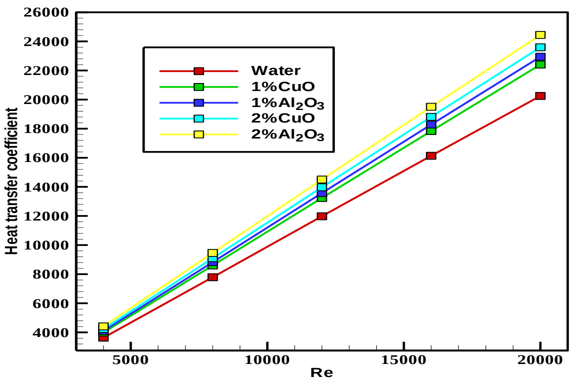

Fig. 6: Variation of the heat transfer coefficient vs Reynolds number

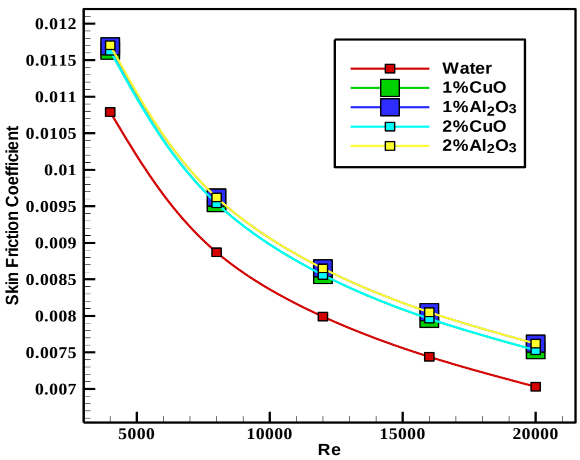

Fig. 7: Variation of the skin friction factor vs Reynolds number

4. Conclusion

In this study, a simulated and numerical study was conducted on a micro coil using a variety of different fluids and nanofluids. The main fluid used was water, with nanofluids such as aluminum oxide and copper (II) oxide. The study focused on measuring the effect of different concentrations for the nanofluids, while different Reynold numbers were incorporated. The results indicated that: Al_2O_3 (aluminum oxide) exhibited to have the highest heat transfer coefficient. It also noted that the velocity and pressure drop were the highest value among the tested fluids, although the friction factor seemed to remain unchanged.
The highest heat transfer coefficient, velocity, wall shear stress and pressure drop increase as the percentage of concentration (φ) increases. Based on the recorded results, there is no direct correlation between the concentration of the particles and friction factor.
The Reynolds number is also recorded to have an effect on the Nusselt number, with a positive correlation. As one increases, so does the other. This also applies to Reynolds number and other properties such as heat transfer coefficient, velocity, and wall shear stress, as well as pressure drop.
The Reynolds number was recorded to have a negative correlation with the friction factor, as the highest Reynolds number led to the recording of the lowest friction factor.
The final conclusion is that the aluminum oxide seems to have the highest effect on the parameters and led to more positive and desirable results. This occurred at a 2% concentration, alongside a 25nm for the dp, using 20000 as the Reynolds number.

Acknowledgement

The authors express gratitude to the Malaysia Ministry of Education (MOE) and Universiti Technologi Malaysia for Research University grant (Q JI30000.2546.19H46)

Nomenclature

Al2O3 Aluminum oxide
Cp Specific heat of the fluid, J/kg K
CuO Copper oxide
df Diameter of base fluid molecule
dp Nanoparticle diameter, m
g Gravitational acceleration, m/s2
k Thermal conductivity, W/m K
keff Effective thermal conductivity
M Molecular weight of base fluid
N Avogadro number, N=6.022×1023mol−1
Nu Nusselt number, Nu=hD/k
P Pressure of fluid, Pa
Pr Prandtl number, Pr=Cp μ/k
Re Reynolds number, Re=ρuD/μ
T Temperature of fluid, K
T Bulk temperature, K
T0 Reference temperature

Greek symbols
μeff Effective viscosity
α Thermal diffusivity, m2/s
μ Dynamic viscosity of fluid, kg/m s
υ Kinematic viscosity of fluid, m2 s
ρ Fluid density, kg/m3
φ Volume fraction of nanoparticles

Subscript
bf Base-fluid
nf Nanofluids
np Nanoparticle
eff Effective

References

[1] Gugulothu, R., Reddy, K. V. K., Somanchi, N. S., & Adithya, E. L. (2017). A review on enhancement of heat transfer techniques. *Materials Today: Proceedings*, *4*(2), 1051-1056.
[2] Yilmaz, M., Comakli, O., Yapici, S. & Sara, O. N. 2003. Heat Transfer and Friction Characteristics in Decaying Swirl Flow Generated by Different Radial Guide Vane Swirl Generators. Energy Conversion and Management 44(2): 283-300
[3] Omidi, M., Farhadi, M., & Jafari, M. (2017). A comprehensive review on double pipe heat exchangers. Applied Thermal Engineering, 110, 1075-1090
[4] Xuan, Y. & Li, Q. 2003. Investigation on Convective Heat Transfer and Flow Features of Nanofluids. Journal of Heat Transfer 125(1): 151-155.
[5] Maïga, S. E. B., Nguyen, C. T., Galanis, N., Roy, G., Maré, T. & Coqueux, M. 2006. Heat Transfer Enhancement in Turbulent Tube flow Using Al2O3 Nanoparticle Suspension. International Journal Numerical Methods Heat Fluid Flow 16(3): 275-292.

[6] Namburu, P. K., Das, D. K., Tanguturi, K. M. & Vajjha, R. S. 2009. Numerical Study of Turbulent Flow and Heat Transfer Characteristics of Nanofluids Considering Variable Properties. International Journal of Thermal Sciences 48(2): 290-302.
[7] Fotukian, S. M. & Nasr Esfahany, M. 2010. Experimental Study of Turbulent Convective Heat Transfer and Pressure Drop of Dilute Cuo/Water Nanofluid inside a Circular Tube. International Communications in Heat and Mass Transfer 37(2): 214-219.
[8] Buongiorno, J. 2005. Convective Transport in Nanofluids. Journal of Heat Transfer 128(3): 240-250.
[9] Demir, H., Dalkilic, A. S., Kürekci, N. A., Duangthongsuk, W. & Wongwises, S. 2011. Numerical Investigation on the Single Phase Forced Convection Heat Transfer Characteristics of Tio2 Nanofluids in a Double-Tube Counter Flow Heat Exchanger. International Communications in Heat and Mass Transfer 38(2): 218-228.
[10] Duangthongsuk, W. & Wongwises, S. 2009. Heat Transfer Enhancement and Pressure Drop Characteristics of Tio2–Water Nanofluid in a Double-Tube Counter Flow Heat Exchanger. International Journal of Heat and Mass Transfer 52(7–8): 2059-2067.
[11] Sajadi, A. R. & Kazemi, M. H. 2011. Investigation of Turbulent Convective Heat Transfer and Pressure Drop of TiO2/Water Nanofluid in Circular Tube. International Communications in Heat and Mass Transfer 38(10): 1474-1478.
[12] Kayhani, M. H., Soltanzadeh, H., Heyhat, M. M., Nazari, M. & Kowsary, F. 2012. Experimental Study of Convective Heat Transfer and Pressure Drop of TiO2/Water Nanofluid. International Communications in Heat and Mass Transfer 39(3): 456-462.
[13] N. Xiao, J. Elsnab, T. Ameel, Microtube gas flows with second-order slip flow and temperature jump boundary conditions, International Journal of Thermal Sciences 48 (2009) 243–251.
[14] J. Koo, C. Kleinstreuer, Viscous dissipation effects in microtubes and microchannels, International Journal of Heat and Mass Transfer 47 (2004) 3159–3169.
[15] A.K. Satapathy, Slip flow heat transfer in an infinite microtube with axial conduction, International Journal of Thermal Sciences 49 (2010) 153–160.
[16] H. Wang, Y. Wang, Influence of three-dimensional wall roughness on the laminar flow in microtube, International Journal of Heat and Fluid Flow 28 (2007) 220–228.
[17] A. Aziz, N. Niedbalski, Thermally developing microtube gas flow with axial conduction and viscous dissipation, International Journal of Thermal Sciences 50 (2011) 332–340.
[18] Vajjha, R. S., D. K. Das and D. P. Kulkarni (2010). "Development of new correlations for convective heat transfer and friction factor in turbulent regime for nanofluids." International Journal of Heat and Mass Transfer 53(21): 4607-4618
[19] Vajjha, R. S. and D. K. Das (2012). "A review and analysis on influence of temperature and concentration of nanofluids on thermophysical properties, heat transfer and pumping power." International journal of heat and mass transfer 55(15): 4063-4078...